

K223: Nuclear $\gamma - \gamma$ angular correlations

Lab Report

Team A5

Aarathi Parameswaran

Purbita Kole

2nd October 2023

Bonn-Cologne Graduate School of Physics and Astronomy

University of Bonn

Advanced Lab Course

Winter Semester 2023/2024

Contents

1	Introduction	1
2	$\gamma - \gamma$ Angular Correlation	2
2.1	Decay Scheme of Co-60	2
2.2	Experimental Considerations	3
2.2.1	Corrections	3
2.2.2	Dependence on the axial distance of the source from the detectors .	4
2.2.3	Dependence on the angle between detectors	4
3	Experimental setup	6
3.1	The fast-slow coincidence and basic circuit components	6
3.2	Setting the Main Amplifiers Gain	8
3.3	Calibration of the SCAs	9
3.4	Finding the CFD threshold	10
3.5	Adjusting the delay in the fast branch	12
3.6	Delay Adjustment in the slow branch	14
4	Angular correlation Measurements and analysis	16
4.1	Measuring Random Coincidences	16
4.2	Measuring Angular correlation	18
4.3	Analysis of Angular correlation	21
5	Conclusion	23
6	Appendix	24
6.1	Correction Factor values	24

1 Introduction

Generally, nuclear spins are expected to have an isotropic distribution, but in non-equilibrium cases, anisotropic behaviour comes up. In this experiment, we have investigated one of such anisotropic distributions of nuclear spin which emerges from the cascaded $\gamma - \gamma$ decay of ${}^{60}_{27}\text{Co}$. Using a circular two-detector setup, we investigated the coincidence count rate at varied emission angles and analytically compared with the theoretical predictions. The main part of this experiment involves measuring coincidence count rates, which is achieved by setting up a fast-slow coincidence circuit. Further, various components of the coincidence circuit have been calibrated and their efficiency has been analysed, for detection of the aforementioned $\gamma - \gamma$ cascade.[1]

2 $\gamma - \gamma$ Angular Correlation

Nuclear systems can decay from an excited state to a stable state and in the process they might emit gamma radiation. If the decay is multilevel, with the intermediate state being a short-lived state (here in the scale of picoseconds), then it is known as a cascaded decay. The probability of emission depends on the angle between nuclear spin and the direction of emission. The expected angular distribution of the emitted photons to be isotropic, but for a cascaded decay it is anisotropic. As it gives rise to electromagnetic multipole radiation which has an anisotropic distribution. [2, 1]

From theoretical considerations, the directional correlation function($W(\theta)$) between two successive γ rays are

$$W(\theta) = 1 + A_{22}P_2\cos(\theta) + \dots A_{k_{max}k_{max}}P_{k_{max}}\cos(\theta) \quad (1)$$

and $k_{max} = \min[2I, 2L_1, 2L_2]$ where I is the nuclear spin of intermediate state and L_i is the order of multi-pole of emitted gamma rays. Thus, each of the coefficients A_{kk} is dependent on the cascade and is obtained from calculating the Clebsch -Gordon or Racah Coefficients for such cascaded gamma decay.

Here we are trying to measure the $\gamma - \gamma$ cascade of $4 - 2 - 0$ decay(decay scheme in terms of nuclear spinof levels). For this decay scheme, the angular correlation function is given by[2]-

$$W(\theta) = 1 + A_{22}\cos^2(\theta) + A_{44}\cos^4(\theta) \quad (2)$$

From the values in [2], for this decay scheme $A_{22} = 0.102$ and $A_{44} = 0.0091$

2.1 Decay Scheme of Co-60

Here we investigate the decay scheme of $^{60}_{27}\text{Co}$ to the stable state of $^{60}_{28}\text{Ni}$. In the decay scheme $4^+ - 2^+ - 0^+$ of ^{60}Co (Fig(1)) we are expected to find two photopeaks at **1.3325 MeV** and **1.1732 MeV**, as these transitions have the highest branching ratio as seen in Fig(1). So the ratio between the energy of the two photopeaks is estimated to be **1.13578**.

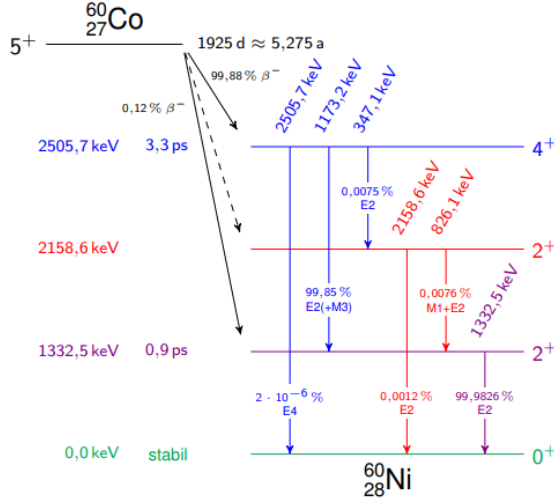


Figure 1: Decay Scheme of $^{60}_{27}\text{Co}$ [1]

2.2 Experimental Considerations

The detected events of coincidences are just averages of true coincidences $W(\theta)$ due to considerations of solid angle limitations of the detector. Experimentally, we also need to measure the true coincidence rate $C(\theta)$. This is done by subtracting the random coincidences rate[2]

$$C(\theta) = C(\theta)_{meas} - C(\theta)_{random} \quad (3)$$

where

$$C(\theta)_{random} = 2\tau_o N_{moving} N_{static} \quad (4)$$

where τ_o is the resolving time of the coincidence unit, N_i are the rates of counts in individual detectors and the resolving time is the resolving time of the coincidence units attached to the two detectors. From here, experimental correlation function can be expressed as $K(\theta) \propto \frac{C(\theta)}{N_{movable}(\theta)}$. So now the function is modified as

$$K(\theta) = K_o[1 + A'_{22}\cos^2(\theta) + A'_{44}\cos^4(\theta)] \quad (5)$$

2.2.1 Corrections

This entire calculation was done considering centred sources and centred point detectors. A larger detector helps to gather more events but would also smear out the angular

correlation. So, a correction to this solid angle limitation of the detector was applied -

$$A_{kk} = \frac{A_{kk}^{exp}}{Q_{kk}} = \frac{A_{kk}^{exp}}{Q_k^2} \quad (6)$$

where Q_{kk} is the product of the correction factor of two individual (Q_k assuming a circular detector both are same) detectors. Q_k is dependent on various factors like the efficiency of detectors, the angle between counter-axis and direction of propagation, the energy of radiation. These values can be calculated based on the said parameters using various methods.

2.2.2 Dependence on the axial distance of the source from the detectors

These corrections will become more significant based on the distance between the source and the detector. We know that the count rate of the detector is given by [2]

$$N(\theta) = Mp_i\epsilon\Omega_i \quad (7)$$

where M is the number of nuclear disintegrations per unit time, p_i is the probability of the disintegration, ϵ is the efficiency of the detector and Ω is the solid angle of the detector which is in turn $\propto \frac{1}{r^2}$ where r is the radial distance between source and the detector. As the Coincidence rate $C(\theta)$ is a product of the two detector counts it is proportional to $\propto \frac{1}{r^4}$ (considering the radial distance of both the detectors to the source remains the same). So the radial distance should be considerably small.

Now looking at the correction factors for a $2'' \times 2''$ detector from [2], we see that for a 4-2-0 cascade that we are measuring here the $Q_2 \geq Q_4$ so Gaussian errors of Q_2 is more significant for the value of A_{kk} . From the table, we see that for the energies 1.5 MeV and 1 MeV (as our photopeaks are 1.33 MeV and 1.17 MeV), correction factors increase for an increase in distance. But the modified coincidence rate will be $\propto \frac{1}{r^4 Q_k^2}$. The error in distance will have a more significant effect, so the distance should be kept at a minimum (5cm here) for this experiment.

2.2.3 Dependence on the angle between detectors

The counts are dependent on the angle and the measuring time is limited. So, we can analyse the behaviour of the correlation function for a 4-2-0 cascaded decay and see which angles have more statistical significance in calculating the correlation function. Comparing

Eq(2) and theoretical values of A_{kk} with Eq(5), one expects the parameters in equation Eq(5) i.e $K_o = 0.9524$, $A'_{22} = 0.125$ and $A'_{44} = 0.04166$. Now for more precise measurements we introduce $\alpha = A'_{22} + A'_{44}$ and $\beta = A'_{22} - A'_{44}$ and express the angular correlation function as

$$f(\theta) = A[1 + \frac{\alpha + \beta}{2}\cos^2(\theta) + \frac{\alpha - \beta}{2}\cos^4(\theta)]$$

So, the expected value of $\alpha = 0.1666$ and $\beta = 0.08333$.

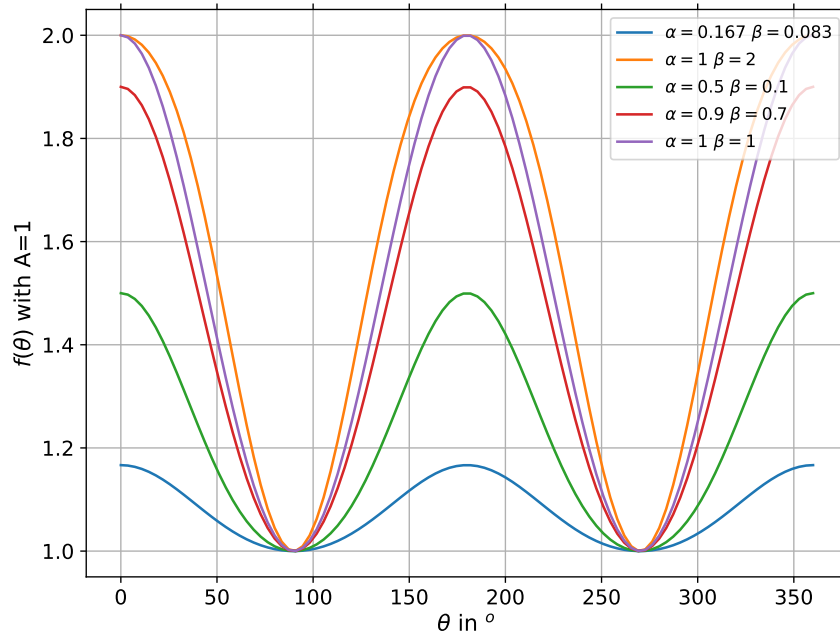


Figure 2: Modified Angular correlation function plotted against the angles for different parameter values

From Fig(2) we can see that function is well defined over the ranges of $90^\circ \rightarrow 270^\circ$. The turning points of the function are at 90° , 180° , 270° , also the points at the FWHM(full-width at half maxima) i.e at 135° and 225° show the biggest change in slope of the curve.

3 Experimental setup

In this experiment, we are utilising **Fast-Slow Coincidence method** to calculate the coincidence rates and calculate the angular correlation of the $\gamma - \gamma$ decays of ^{60}Co . This circuit helps in timing and determining whether the counts from events are coincident and is suitable for measuring angular coincidences from two different detectors. In a coincidence technique, an output is produced if there is an overlap of the incoming signals. In the fast-slow technique, the signal is divided into a slow branch and a fast branch and goes into a three-fold coincidence unit [3].

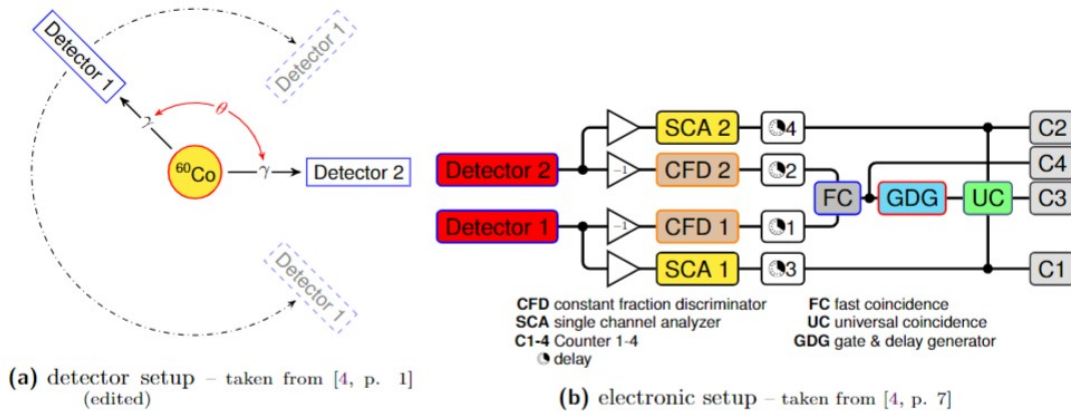


Figure 3: Schematic of the setup of the experiment [1]

3.1 The fast-slow coincidence and basic circuit components

The circuit is comprised of various components and the function of each component is crucial for the setup. The basic function of each component is stated here to supplement the experimental setups[3].

1. **Amplifier** An amplifier increases the magnitude of the input signal with a certain gain, which is the ratio between the input and output signal.

2. Delay amplifier

A delay amplifier adds an adjustable delay to the circuit. In the nanosecond regime, this can be realized simply with a varying cable length, for longer delay times one can use a capacitor. By converting the signal to a current and storing it in a capacitor, the discharging time can be varied.

3. **Constant fraction discriminator** A CFD creates a threshold, which has to be overcome by the input signal to get an output, it is used for example to remove noise. However, the input and output signals are usually time-shifted, whereby the shift is not independent of the input signal. Therefore the CFD does the following. It splits the signal into two parts, one is delayed and the other one is inverted. The threshold value is connected to the inverted signal. After that, the two parts are added together again, after adding them the combined signal has a zero-crossing point which is independent of the amplitude of the input signal.
4. **Single channel analyzer** A SCA is simply a device (basically it is also a discriminator) that gives an output signal only if the input signal is in the range between the upper and lower limit of the SCA. The SCA is a discriminator which sorts input signals according to their amplitude. A standard logic signal output is created only if the input signal falls in the region between the lower and upper threshold (the window) of the SCA.
5. **Multi channel analyzer** A MCA sorts all input signals in different channels and then gives an output.
6. **Coincidence unit** The coincidence unit takes multiple, in our case two, input signals and gives only then an output signal, if the two input signals arrived simultaneously, or at least in a given time span.
7. **GDG** A gate delay generator is a device which generates variable width gate pulses ranging from a few nanoseconds to seconds. It is usually triggered by an input signal or manually and is used to activate a certain device and is used as a timer.

3.2 Setting the Main Amplifiers Gain

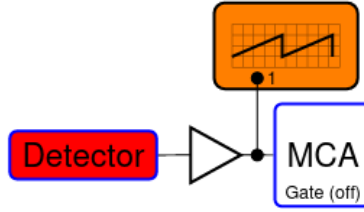
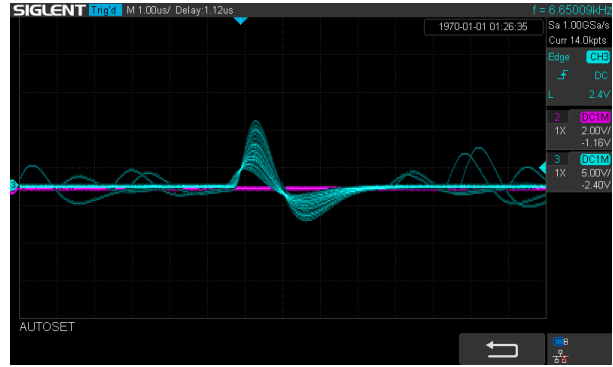


Figure 4: Circuit diagram for setting the amplifier gain [1]

The first step is to adjust the gain of the main amplifiers to have the amplitude of the signal output be as high as we require it to be.



Amplifier output for the left detector

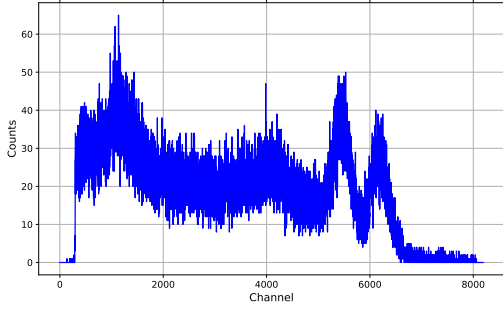


Amplifier output for the right detector

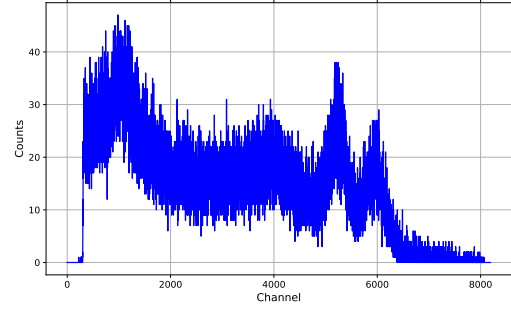
Figure 5: Amplifier output for gain adjustment

Figure(5) shows the oscilloscope screen after the adjustment of the gain. The adjustment of amplification was done till the height of the signals (the amplitudes of the photopeaks) on the oscilloscope roughly corresponded to 8-9V, which is as expected. The output of the amplifiers is linear up to 9V, and the maximum signal amplitude of the electronics is 10V [1].

The shape of the signal is as expected with a fast rise and slower fall after the peak. For a saturated signal, the peak would become a plateau at the maximum.



Measured spectra from left detector



Measured spectra from right detector

Figure 6: Measured Spectra from both detectors after setting amplifier gain

From the measured spectra in figure(6), we can see the required photopeaks which are roughly at the same position for both detectors.

3.3 Calibration of the SCAs

The next step is to set the thresholds of the SCAs so that they select required pulses the correspond to the photopeaks of the spectrum. The signal from the detector from the amplifier is then put into an SCA. The signal from the SCA is passed through the GDG and input into the gate of the MCA and visualised on the oscilloscope. The GDG delay is set such that photopeaks are roughly in the middle of the SCA output. The SCA is operated in window mode, where a window region is defined and the lower limit is changed, allowing an even scan of the spectrum. The spectrum is measured twice, once using the internal gate and once with the SCA gate. Adjusting this threshold, we perform the cuts required to select only the regions with the photopeaks with minimal noise. The chosen cuts and threshold for both the fixed and movable detectors (left and right) can be seen in figure(8).

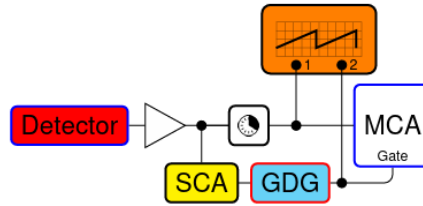


Figure 7: Circuit diagram for adjusting SCA threshold [1]

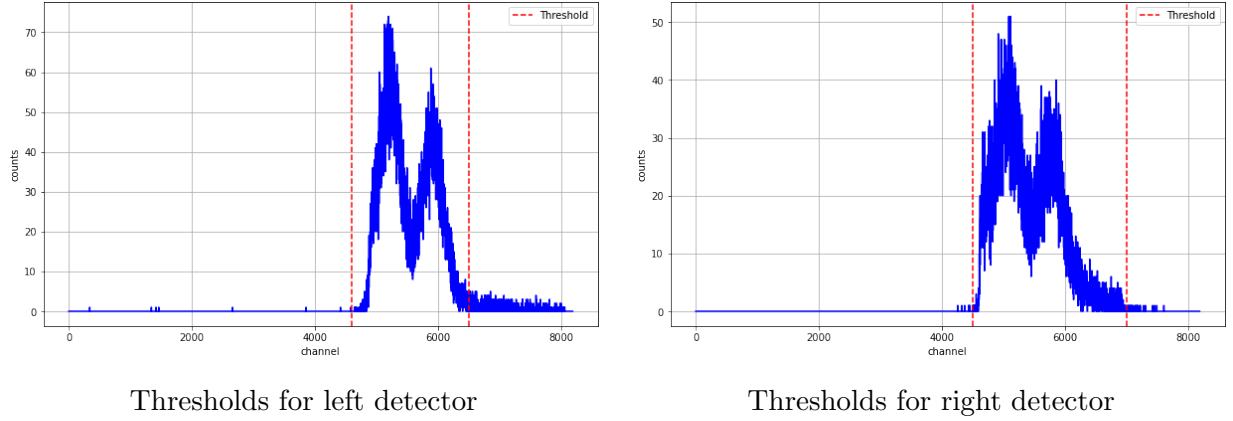


Figure 8: SCA thresholds for both detectors

The sensitivity of the SCA in dependence of the energy is given by the equation

$$\eta_{SCA,i}(E) = \frac{N_{SCA-gated}(E)}{N_{self-gate}(E)} \quad (8)$$

This quantifies the quality of our selected thresholds. Normalising the data and calculating the sensitivity using the above equation, the plots are obtained as seen in figure(9) and as expected the sensitivity is close to 1 at the channels where the photopeaks were observed.

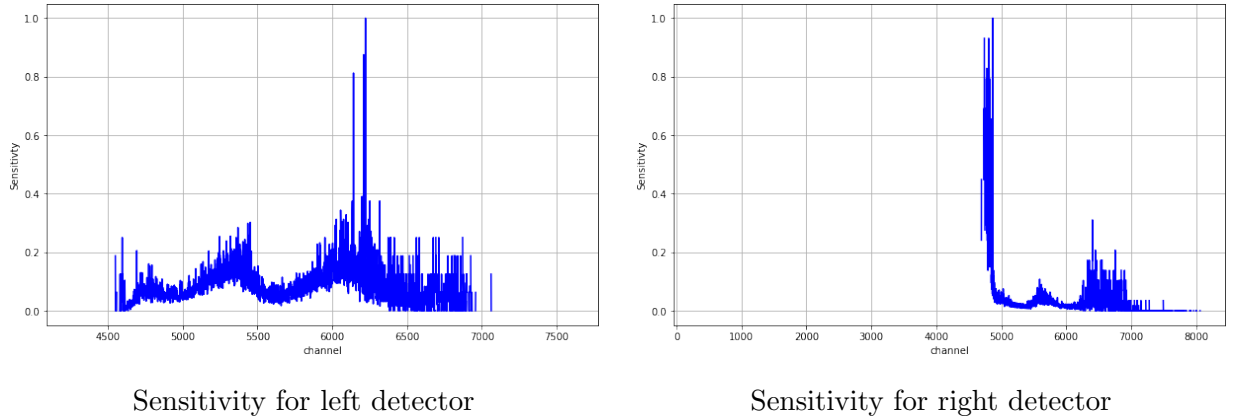


Figure 9: SCA sensitivity for both detectors

3.4 Finding the CFD threshold

The CFD threshold also needs to be set to further filter out the noise from the actual signal.

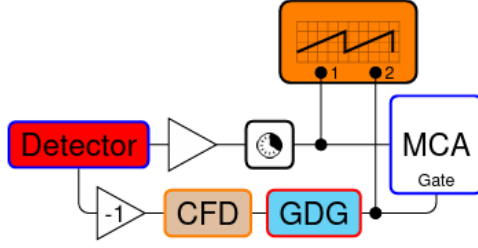


Figure 10: [1]

The measured spectra after selecting the thresholds are plotted in a logarithmic y scale as seen in figure(11). As in the case of the SCA, we measure the spectra twice, once with the internal gate and once with the CFD gate. We were not able to perform the right cut as accurately as we would've liked, which is why there is some amount of noise there, possibly due to a low set threshold.

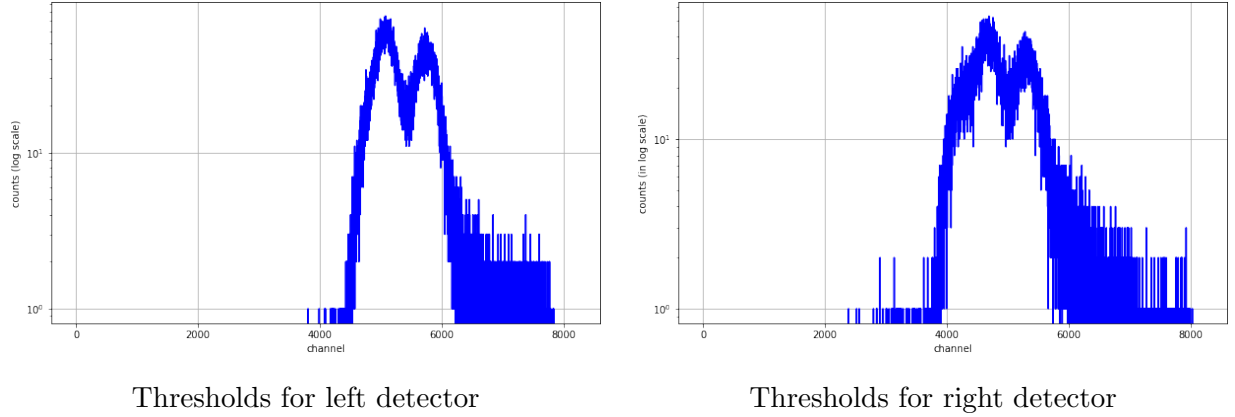


Figure 11: CFD thresholds for both detectors

The sensitivity of the CFD can then be calculated using the equation

$$\eta_{CFD,i}(E) = \frac{N_{CFD-gated}(E)}{N_{self-gate}(E)} \quad (9)$$

The data was normalized and the sensitivity was calculated for each of the channels using the above equation to obtain the following plots. The effect of the threshold close to the second photopeak can be seen in the plot for the sensitivity, with higher noise on the right.

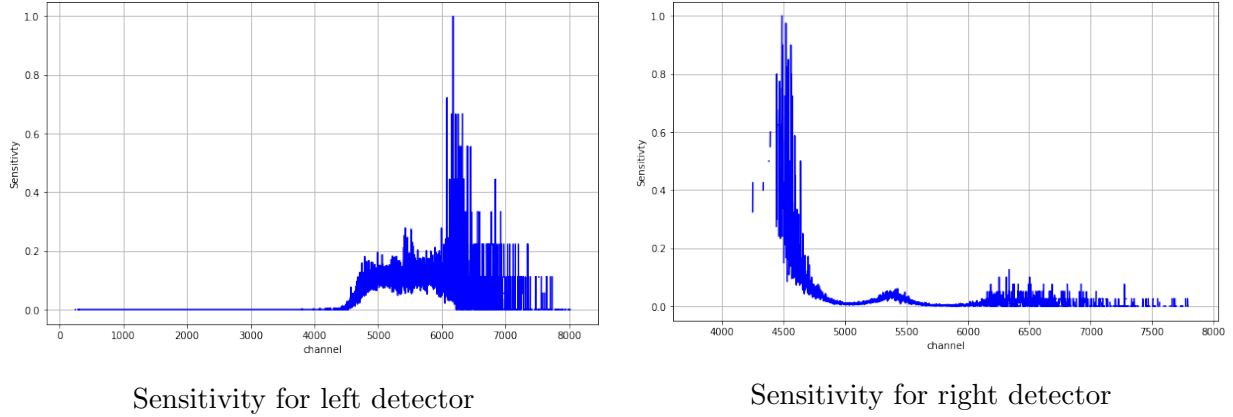


Figure 12: CFD sensitivity for both detectors

As seen in figure(12), the sensitivity of the CFD is almost at 1 near the region of interest, which are the channels with the photopeaks.

3.5 Adjusting the delay in the fast branch

This step involves finding an optimal delay setting for the fast branch of the circuit. This is done to make sure that the output signals of both the CFDs are in coincidence at the fast coincidence module. Delay 1 in figure(13) is set to a fixed value and Delay 2 is changed in steps and the counts of the fast coincidence module are measured.

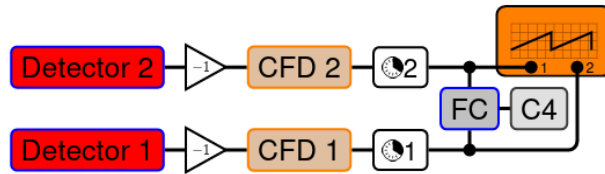


Figure 13: Circuit diagram to setup delay in the Fast Branch [1]

The data obtained is then fit to a function:

$$f(t) = \frac{A}{2} \left(1 + \operatorname{erf} \left(\frac{t - (t_0 - \frac{w}{2})}{\sigma} \right) \operatorname{erf} \left(\frac{(t_0 + \frac{w}{2}) - t}{\sigma} \right) \right) + A_0 \quad (10)$$

Here, A is the amplitude, A_0 is the constant background (baseline), σ is the standard deviation which depicts the steepness of the curve, t_0 is the delay for which the highest coincidence is observed for the signals (the center of the profile) and w is the width of the

curve which depicts the resolving time. We require the resolving time to be short enough to reduce random coincidences but long enough to ensure that the true coincidences are detected.

The measured values and the fit performed to it can be seen in figure(14).

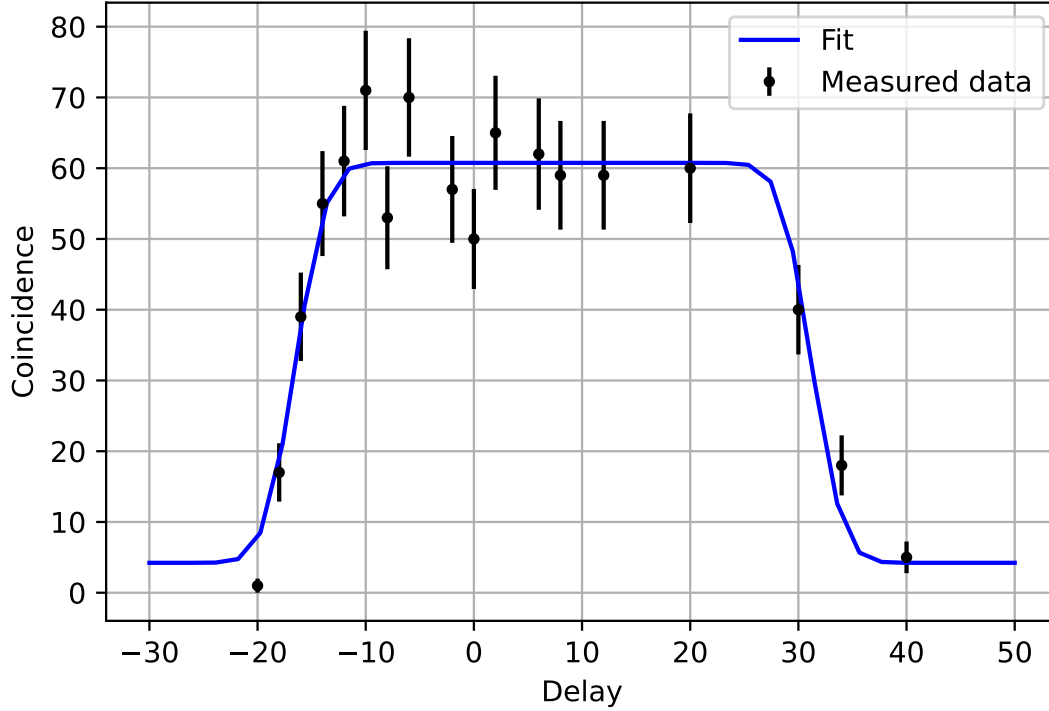


Figure 14: Prompt Curve

The width of the function is determined by w , so a larger resolving time would lead to a broader function and a smaller w results in a narrower profile.

The width of the slopes would be the steepness of the curve which is determined by the standard deviation σ . Smaller σ would lead to steeper slopes at the edges while larger σ would lead to wider slopes.

If the resolving time is too short, the profile of the prompt curve will become narrow, while a larger resolving time would result in a wider profile. The obtained values for the parameters from the fit can be seen in table(1).

Table 1: Parameter Values and Errors

Parameter	Value	Error
A	56.52	6.18
A_0	8.46	11.46
t_0	7.37	0.40
w	47.70	1.18
σ	3.2	0.98

3.6 Delay Adjustment in the slow branch

This step involves ensuring that the signals from the SCA and the fast branch are in coincidence at the universal coincidence module. The circuit is as seen in figure(15).

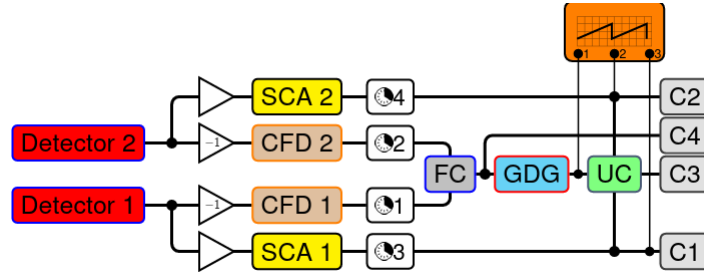


Figure 15: Circuit to adjust the delay in the Slow Branch [1]

This is done by triggering the outputs and adjusting the SCA delays. The GDG width is adjusted to make all the peaks nearly the same length. By looking at the display on the oscilloscope, can verify that the three signals are in coincidence (figure(16)). The three signals seen here are the two SCA output signals and the output of the fast circuit from the GDG. We tried to align the signals using the center to ensure that there was a long overlap, as the signals were not steady and aligning the edges would have been more difficult.

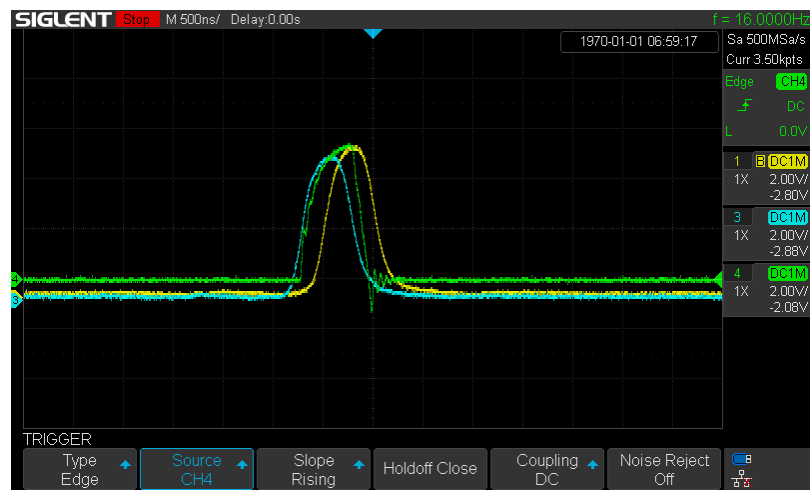


Figure 16: Adjustment of the Slow coincidence: coincidence as seen on the oscilloscope

4 Angular correlation Measurements and analysis

This setup of the fast-slow coincidence will now be utilised in measuring angular coincidences. The counts and coincidences of two detectors were measured for **48 hrs**, with a number of measurements for varying angles (θ) between the detector from 90° to 270° . Each measurement included θ values at a step of 15° , and measurement for each angle was done for **$599.99 + \pm 0.5$ s** on an average. The distance between the source and the detectors was found to be

- $r_{\text{moving}} = 46.02 \pm 0.05 \text{ cm}$

- $r_{\text{static}} = 46.16 \pm 0.05 \text{ cm}$

The peaks to be observed have an average energy $E \approx 1.2\text{MeV}$.

4.1 Measuring Random Coincidences

Before starting with the main measurements, one needs to determine the random coincidences in the setup. This is done by measuring coincidences outside the resolving limit of the setup, i.e. in Fig(14) in the non-plateau region. So, a **60 ns** delay was chosen for the fast circuit, and measurements were taken for different angles between 90° and 270° for about **50 mins**. The average integration time for each measurement was **$120 + \pm 0.2$ s** on average.

Changing the delay only in the fast branch might lead to an error as the slow circuit is modified to acquire coincidences within the same resolving time. But this does not lead to a substantial error as long as the coincidences are measured well outside the plateau region and we have selected quite a large value of delay for the fast circuit to avoid any true coincidences.

In Fig(17), despite the nearly constant static count rates observed throughout the measurement duration, we see significant deviations for the moving detector.

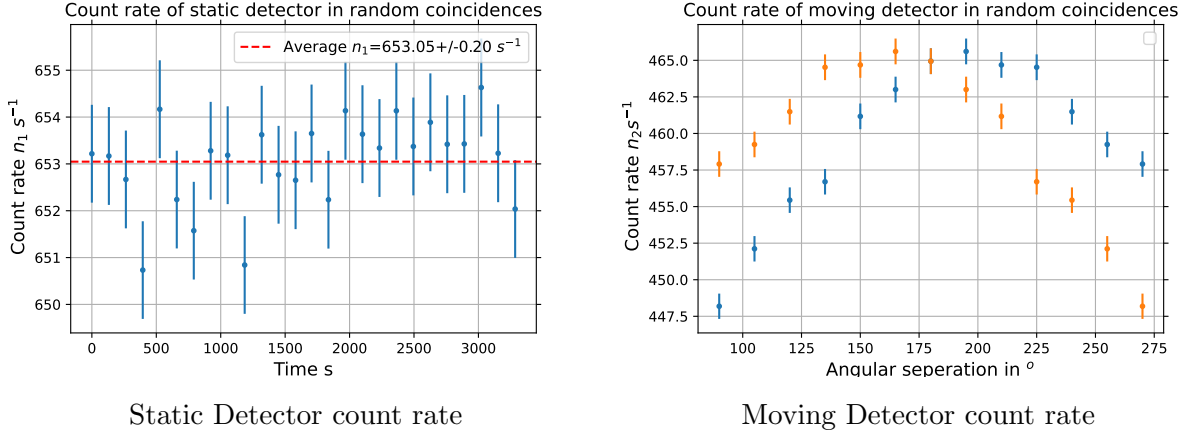


Figure 17: Detector Count rates for random coincidences measurement

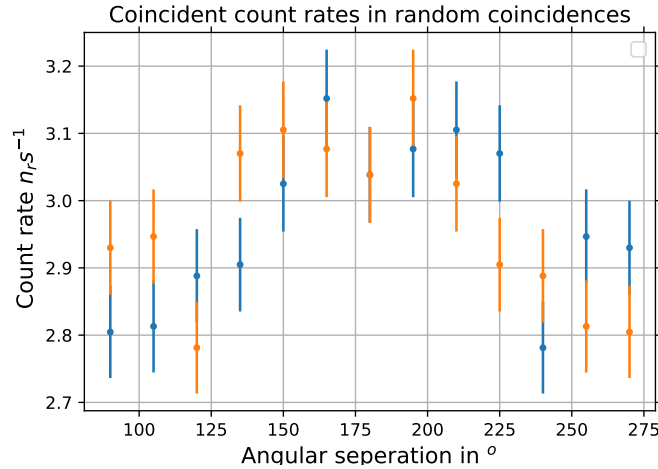


Figure 18: Coincidence rate measured for various angles at random coincidence

From the data, the total count of coincidence for each angle in each individual measurement and their integration time was taken. The Gaussian errors of the data were calculated as \sqrt{N} , where N is the no of counts. The total number of coincidences over the entire measurement (N_r) was found to be 46270.0 ± 215.10462 . Then, the coincident rate was calculated to be $\mathbf{n_r} = \frac{N_r}{T(\text{total integration time})} = \mathbf{2.966 \pm 0.014 \text{ s}^{-1}}$. The error is calculated from the Gaussian error and was executed in Python using the package `Uncertainties`[4].¹ Theoretically, the coincidence rate can also be calculated from the count rates of the two

¹All the Gaussian error calculations from here on were done using the `Uncertainties` package

detectors using Eq(4). The resolving time from Table(1), is 47.70 ± 1.18 ns and from random coincidences the count rate of both moving and static detector was determined. From there, the theoretical coincidence rate are calculated as $(n_{r_{\text{theo}}}) = 2.85 \pm 0.07$ s⁻¹. So the two values agree well. This n_r value is subtracted from the coincidence counts of the main measurement.

4.2 Measuring Angular correlation

Now the main measurement is performed using the parameters mentioned before and about 16 full measurements were taken.

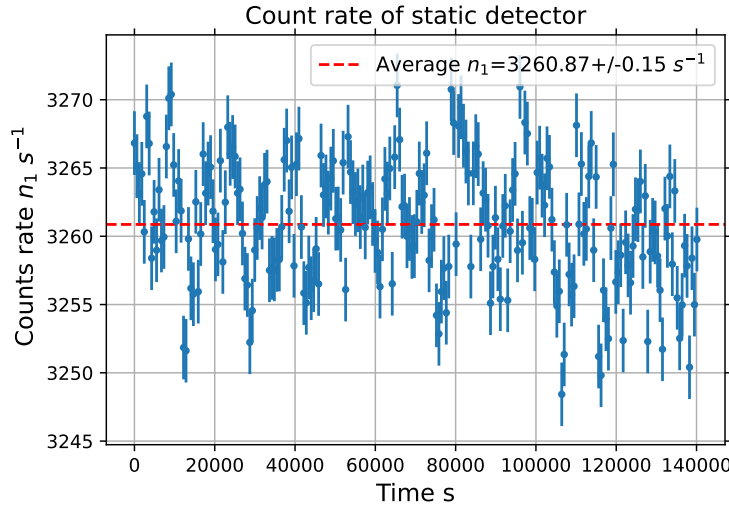


Figure 19: Count rate of static detector over measurement time for true coincidences

As seen in Fig(19), the count rate of static detector fluctuates around 3260.87 ± 0.15 s⁻¹. The moving detector count rate for each angle varies with measurements i.e. it drifts with time. This can be seen in Fig(20), where the initial 2 measurements show considerably lower count rates. In later measurements, the fluctuations of the count rate are quite stable.

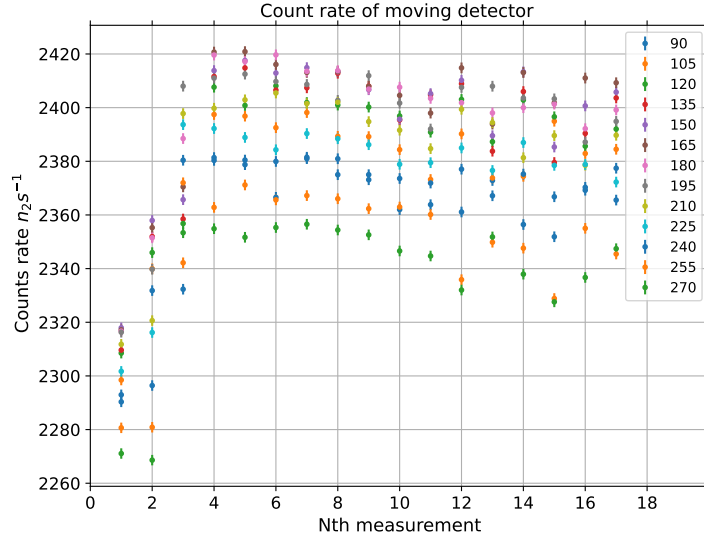


Figure 20: Count Rate of Moving Detector at various angles throughout all measurements

The fast coincidence rate and the angular coincidence rate are quite stable over time for each angle as seen in Figs(21,22). The slight drift in values over all measurements is due to the instability of electronic overtime[1].

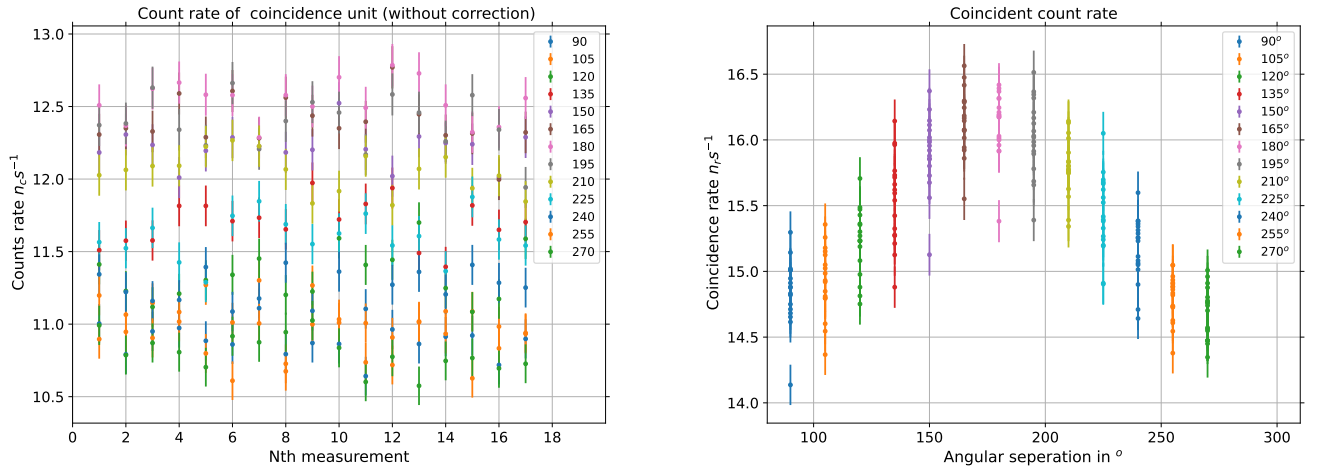


Figure 21: Coincidence Count rate for different angles

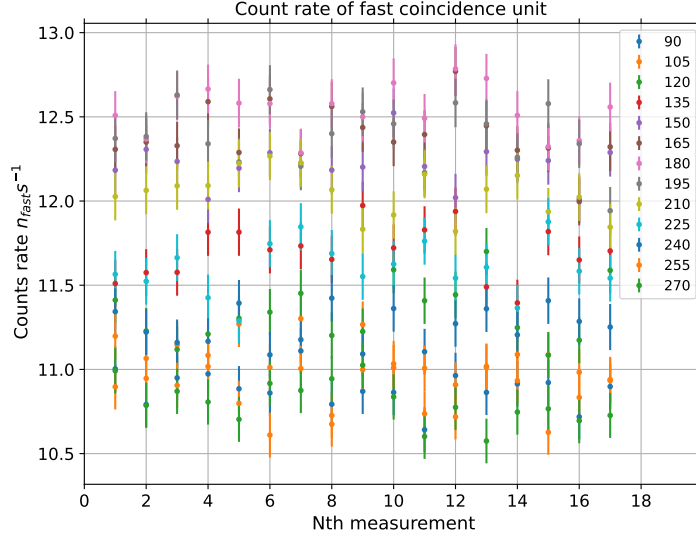


Figure 22: Fast Coincidence count rate overall measurements at different angles

From the values in Fig(21), the total coincidence count rate (n_c) was determined. The random coincidences rate (n_r) calculated before, was subtracted from it. But still, an error might remain from solid angle correction or misalignment of setup. So to get the experimental correlation function we multiply by a correction factor $k(\theta) = \frac{N_{moving}(180^\circ)}{N_{moving}(\theta)}$. So the total correction on the coincidence count rate can be given as

$$K(\theta) \propto n_{c_{corr}} = (n_c - n_r) \frac{N_{moving}(180^\circ)}{N_{moving}(\theta)}$$

$N_{moving}(180^\circ)$ is used to normalise the data with respect to a fixed count rate(here the average of the count rates at 180° is taken). The obtained $K(\theta)$ value was fitted with the angular correlation function given in Eq(5). The fit can be seen in Fig(23). The χ^2 score of the fit was calculated and found to be **0.0031** which implies that the fit results match well with the data. But such significantly low χ^2 score may also signify over-fitting[5].²

²The χ^2 score was calculated using the formulae $\chi^2 = \sum \frac{N(\text{observed}) - N(\text{expected})^2}{N(\text{expected})}$ [5]

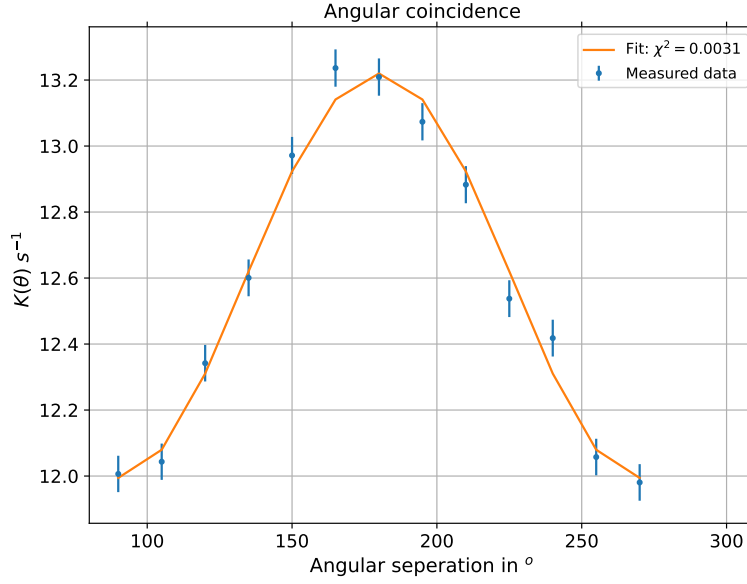


Figure 23: Angular Correlation function over different angles

K_o	A'_{22}	A'_{44}
12.008 ± 0.0004	0.103028 ± 0.00009	0.05271 ± 0.0078

Table 2: Parameters of the fit of the angular correlation based on 4-2-0 cascaded decay

4.3 Analysis of Angular correlation

Now we need to correct the angular correlation for the solid angle error of detectors(as described in Sec(2.2.1)).

E(Mev)	Q_2	Q_4
1.0	0.9046	0.7086
1.5	0.9057	0.7114
Average value	0.9258	0.7100

Table 3: Correction factors obtained for a 2" \times 2" crystal for a radial distance of 5cm (Appendix(6.1))

So the correlation coefficients are divided by Q_k^2 , i.e. the square of the correction factors

obtained from Table(3). The actual correlation values were then found to be

$$\mathbf{A}_{22}^{\text{corr}} = 0.12429 \pm 0.000311 \quad \mathbf{A}_{44}^{\text{corr}} = 0.08 \pm 0.04$$

The expected values as derived from [2] and mentioned in Sec(2.2.3) are $A'_{22} \approx 0.125$ and $A'_{22} \approx 0.04166$. The values match well within their error range. Thus we can verify that the coincidences were from a quadrupole-quadrupole interaction of a $4 - 2 - 0$ cascade of ^{60}Co .

To eliminate the possibility of the correlation belonging to any other cascade of a similar kind, angular correlation was also fitted with angular correlation curves from other cascades. The correlation function for a $0-1-0$ and a $\frac{1}{2} - \frac{3}{2} - \frac{1}{2}$ cascade which were fitted to the data, are given respectively by[2]-

$$K(\theta)_{0-1-0} = K_o^{0-1-0} [1 + \frac{1}{2} Q_2^2 \cos^2(\theta)] \quad K(\theta)_{\frac{1}{2}-\frac{3}{2}-\frac{1}{2}} = K_o^{\frac{1}{2}-\frac{3}{2}-\frac{1}{2}} [1 + \frac{1}{4} Q_2^2 \cos^2(\theta)]$$

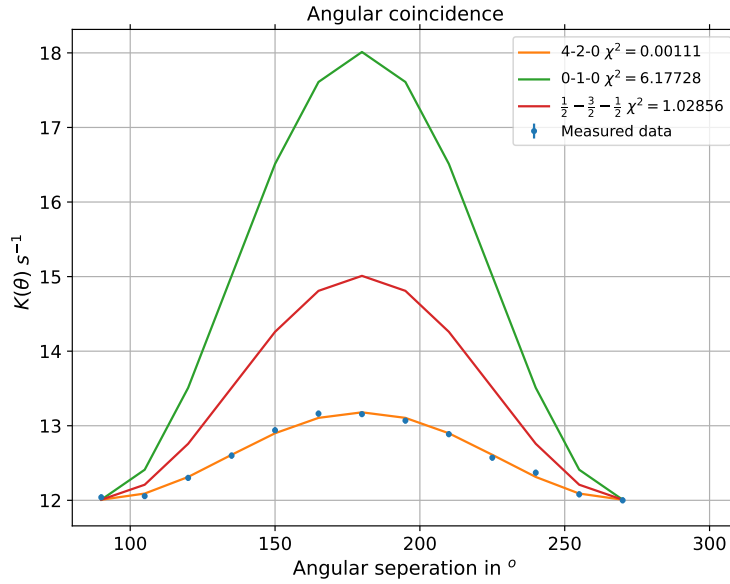


Figure 24: Angular Correlation Function data fitted for the theoretical predictions of other cascades

As seen from Fig(24), the other angular correlation function for other cascades do not overlap with our data and also the χ^2 score for the fits are quite high. So, we can safely conclude that the data for the angular correlation function does not belong to other similar types of cascade decay of an even-even nucleus.

5 Conclusion

In this experiment, the γ - γ decay cascade of ^{60}Co was investigated and the angular correlations were measured. This involved the setting up of a Fast-Slow coincidence circuit and calibrating the individual components and the circuits to make the measurements reliable. This included calibrating and finding thresholds for the SCA, CFD and adjusting delays to set up the coincidence for the fast and slow branches.

In measuring the angular coincidences, at first, the random coincidences of the detector were subtracted from the data of true coincidences. Then the data for true coincidences were also corrected for limitations of solid-angle. The data was fitted for $4 - 2 - 0$ cascaded decay at energies between $1 - 1.5$ MeV, with the radial distance between detector and source being 5cm(which is very close to the distance in our experiment, which is ≈ 4.6 cm). From the fit of a χ^2 value **0.0031**, the correlation function coefficients were found to be

$$\mathbf{A_{22}^{corr} = 0.12429 \pm 0.000311 \quad A_{44}^{corr} = 0.08 \pm 0.04}$$

The possibility of this data being a signature of other similar types of cascade was also shown to be statistically insignificant, from fit parameters.

Higher accuracy in random coincident rate could have been achieved by taking longer measurements and using a more suitable delay length for the fast setup. For the main measurement, more accurate data could have been measured, if the measurement was optimised to measure longer at the crucial angles.

6 Appendix


6.1 Correction Factor values

Correction factors for $2'' \times 2''$ crystals.
Calculated by E. Matthias using the present programme

h (cm)	E (MeV)	ϵ		Q_2		Q_4	
		Whole spectrum	Photopeak	Whole spectrum	Photopeak	Whole spectrum	Photopeak
10.0	1.5	0.4163	0.1108	0.9657	0.9692	0.8888	0.8999
	1.0	0.4781	0.1648	0.9653	0.9686	0.8876	0.8979
	0.7	0.5417	0.2449	0.9649	0.9678	0.8861	0.8955
	0.5	0.6116	0.3539	0.9642	0.9671	0.8842	0.8933
	0.3	0.7523	0.6167	0.9624	0.9643	0.8785	0.8845
	0.2	0.8640	0.8103	0.9597	0.9607	0.8700	0.8732
	0.15	-	-	0.9576	0.9576	0.8635	0.8646
	0.10	0.9694	0.9603	0.9557	0.9557	0.8573	0.8575
	0.05	0.9950	0.9933	0.9545	0.9545	0.8538	0.8538
	0.03	0.9907	0.9869	0.9547	0.9547	0.8544	0.8544
	0.02	0.9971	0.9958	0.9544	0.9544	0.8535	0.8535
7.0	1.5	0.3796	0.0993	0.9378	0.9440	0.8032	0.8222
	1.0	0.4375	0.1485	0.9369	0.9441	0.8006	0.8225
	0.7	0.4976	0.2202	0.9359	0.9422	0.7976	0.8167
	0.5	0.5648	0.3265	0.9346	0.9403	0.7935	0.8109
	0.3	0.7055	0.5736	0.9306	0.9345	0.7815	0.7932
	0.2	0.8288	0.7757	0.9246	0.9265	0.7636	0.7694
	0.10	0.9599	0.9507	0.9152	0.9153	0.7358	0.7363
	0.05	0.9934	0.9917	0.9124	0.9124	0.7278	0.7278
	0.03	0.9877	0.9839	0.9129	0.9129	0.7292	0.7293
	0.02	0.9961	0.9948	0.9122	0.9122	0.7272	0.7272
5.0	1.5	0.3472	0.0925	0.8947	0.9057	0.6801	0.7114
	1.0	0.4014	0.1421	0.8930	0.9046	0.6754	0.7086
	0.7	0.4584	0.2017	0.8911	0.9016	0.6699	0.7001
	0.5	0.5230	0.3007	0.8885	0.8981	0.6626	0.6901
	0.3	0.6633	0.5366	0.8808	0.8879	0.6411	0.6612
	0.2	0.7963	0.7439	0.8693	0.8727	0.6094	0.6188
	0.10	0.9510	0.9419	0.8503	0.8505	0.5587	0.5593
	0.05	0.9919	0.9902	0.8444	0.8444	0.5436	0.5436
	0.03	0.9850	0.9813	0.8455	0.8455	0.5462	0.5463
	0.02	0.9952	0.9939	0.8439	0.8439	0.5423	0.5424

Figure 25: Solid-angle correction factor for crystal scintillation detector [2]

References

- [1] *Nuclear gamma-gamma Angular Correlations*. English. University of Bonn.
- [2] K. Siegbahn. *Alpha- Beta- and Gamma-ray Spectroscopy*. Alpha- Beta- and Gamma-ray Spectroscopy v. 2. North-Holland Publishing Company, 1965. URL: <https://books.google.de/books?id=4r7QAAAAMAAJ>.
- [3] William R. Leo. *Techniques for Nuclear and Particle Physics Experiments*. Springer Berlin Heidelberg, 1994. DOI: [10.1007/978-3-642-57920-2](https://doi.org/10.1007/978-3-642-57920-2). URL: <https://doi.org/10.1007/978-3-642-57920-2>.
- [4] Ericnbs; O. LEBIGOT. *Welcome to the uncertainties package*. URL: <https://pythonhosted.org/uncertainties/>.
- [5] R.J. Barlow. *Statistics: A Guide to the Use of Statistical Methods in the Physical Sciences*. Manchester Physics Series. Wiley, 1993. ISBN: 9780471922957. URL: <https://books.google.de/books?id=qqKgx47QMX8C>.